International Journal of Medical, Medicine and Health Sciences
ISSN: 2517-9969
Vol:1, No:2, 2007

Effect of Non-Newtonian Behaviour of Blood on Pulsatile Flows in Stenotic Arteries

Somkid Amornsamankul, Benchawan Wiwatanapataphee, Yong Hong Wu, Yongwimon Lenbury

***Abstract*—** In this paper, we study the pulsatile flow of blood through stenotic arteries. The inner layer of arterial walls is modeled as a porous medium and human blood is assumed as an incompressible fluid. A numerical algorithm based on the finite element method is developed to simulate the blood flow through both the lumen region and the porous wall. The algorithm is then applied to study the flow behaviour and to investigate the significance of the non-Newtonian effect.

***Keywords*—** stenotic artery, finite element, porous arterial wall, non-Newtonian model.

I. Introduction

FOR many decades, cardiovascular disease has been one of the most severe diseases causing a large number of deaths worldwide each year, especially in developed countries. Most of the cases are associated with some form of abnormal flow of blood in stenotic arteries. In the presence of a stenosis, the normal blood flow through the artery is disturbed resulting in blood recirculation and wall shear stress oscillation near the stenosis. The heart has to increase the blood pressure to impel the blood passing through the narrowing region so as to enforce the blood circulation. If the heart works too hard and the blood cannot flow well, heart attack may occur.

In order to understand the blood flow behaviour in arteries so as to provide sufficient information for clinical purposes, intensive research has been carried out worldwide for both normal and stenotic arteries [1], [2], [3], [4], [5], [6]. Most analyses assumed the human blood to be Newtonian and the stenoses to be symmetric to make the problem more traceable [7], [8]. Various mathematical models and finite element based numerical methods have been developed to simulate blood flow through the stenotic arteries, including two-dimensional and three dimensional Newtonian models and non-Newtonian models [9], [10], [11], [12].

Althrough a large number of studies have led to better understanding of the flow behaviour induced by a stenosis, further analysis and development are still needed to accurately simulate blood flow under different conditions. One of the important aspects, in simulating blood flow, is to accurately describe the nature of blood as a fluid. It has been generally accepted that blood behaves as a Newtonian fluid when the shear rate is greater than $100s^{-1}$ [13], [14], [15]. However, when the shear rate is lower than $100s^{-1}$, blood behaves as a non-Newtonian fluid and the stresses depend nonlinearly on the deformation rate. Many models assume blood flow to be Newtonian, however, the instantaneous shear rate over a cardiac cycle may vary from zero to over $1000s^{-1}$ depending on the circumstance. Therefore, it is useful to study the significance of non-Newtonian effect on pulsatile blood flows. Hence, the aims of this study are two fold : to develop a finite element model to study the behaviour of blood flow through stenotic arteries taking into account of blood transport through the porous arterial wall, and to investigate the effect of non-Newtonian viscosity of blood on pulsatile flow through an artery with an asymmetric or a symmetric stenosis over a cardiac cycle.

Manuscript received March 20,2006. This work was supported by the Royal Thai Government, the Commission On Higher Education and the Australian Government through the 2005 Australia Endeavour Chueng Kong Award.

S. Amornsamankul and Y-H. Wu are with the Department of Mathematics and Statistics, Curtin University of Technology, WA 6100 Australia (corresponding author phone: 618-9266-3142; email:somkid.amornsamankul@postgrad.curtin.edu.au).

B.Wiwatanapataphee and Y. Lenbury are with the Department of Mathematics, Mahidol University, Bangkok 10400 Thailand.

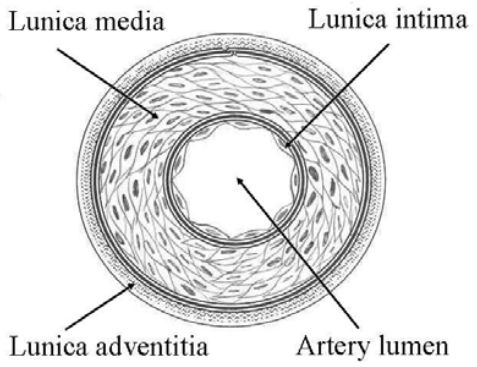

Fig. 1. A cross section of the arterial vessel.

II. Mathematical Model

A blood vessel consists of several layers as shown in Fig. 1. Blood is transported mainly through the lumen but some could be transported through the porous layers including the lunica intima and lunica medium layers. In the lumen region, the equations governing the flow of blood include the continuity equation and the Navier-Stokes equations :

$$\nabla \cdot \mathbf{u} = 0, \tag{1}$$

TABLE I
VALUES OF PARAMETERS USED IN COMPUTATIONAL REGION

n	α_n^Q	θ_n^Q	α_n^p	θ_n^p
1	17.28	2.256	-21.740	-0.406
2	-34.91	-0.226	-9.088	0.202
3	-16.11	1.228	4.771	-0.633
4	11.70	4.882	2.035	-4.315
5	6.64	-0.074	0.768	3.932

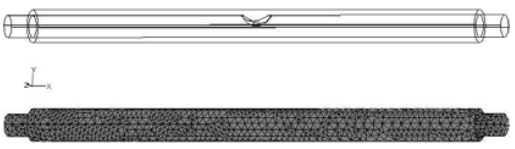

Fig. 2. The 3-D geometry of the 50% stenotic tubes and its finite element mesh.

$$\rho\left(\tfrac{\partial \mathbf{u}}{\partial t}+\mathbf{u}\cdot\nabla\mathbf{u}\right)=-\nabla p_1+\nabla\cdot\left(\mu_n\left(\nabla\mathbf{u}+(\nabla\mathbf{u})^T\right)\right)+\mathbf{f}, \tag{2}$$

where ρ denotes the blood density, $\mathbf{u}=(u_1,u_2,u_3)$ is the velocity vector, $\mathbf{f}=(f_1,f_2,f_3)$ is the volume force acting on the fluid, p_1 denotes pressure in the luminal channel, and μ_n is the viscosity of blood. For Newtonian fluid, μ_n is taken to be a constant. For non-Newtonian fluid, μ_n is a function of shear rate $\dot{\gamma}=\sqrt{2\mathbf{D}:\mathbf{D}}$ where

$$\mathbf{D}\ =\ \frac{1}{2}(\nabla\mathbf{u}+(\nabla\mathbf{u})^T)$$

denotes the rate of deformation tensor. In this study we use the Carreau model for blood, namely

$$\mu_n=\mu_\infty+(\mu_0-\mu_\infty)[1+(\lambda\dot{\gamma})^2]^{(n-1)/2},$$

where μ_0, μ_∞, λ, and n are constants.

In the porous layer of the arterial wall, the flow of blood is described by the continuity equation and the Brinkman equations :

$$\nabla\cdot\mathbf{v}\ =\ 0, \tag{3}$$

$$\rho\frac{\partial\mathbf{v}}{\partial t}+\frac{\mu}{\kappa}\mathbf{v}\ =\ -\nabla p_2+\nabla\cdot\left(\mu\left(\nabla\mathbf{v}+(\nabla\mathbf{v})^T\right)\right)+\mathbf{g}, \tag{4}$$

where μ denotes the viscosity of blood in the porous layer, κ is the permeability of the porous media, $\mathbf{v}$ represents the velocity vector, p_2 denotes pressure in the wall, and $\mathbf{g}$ is the volume force acting on the fluid in the wall.

To precisely describe the cyclic nature of the heart pump and the pulsatile flow condition in the arteries, we use Fourier series to represent the pulsatile pressure and flow rate in the arteries. Therefore, we impose a pulsatile flow rate condition on the inlet boundary and a corresponding pulsatile pressure condition on the outlet boundary of the computational region, namely, for $i,j=1,2,3$

$$\begin{aligned}
u_1=\bar{u}_0(t)&=\tfrac{1}{A}[\bar{Q}+\textstyle\sum_{n=1}^5\alpha_n^Q cos(\frac{2n\pi t}{T}-\theta_n^Q)],\\
u_2=u_3&=0 \qquad\qquad \text{on } \partial\Omega_{in}\\
p&=\bar{p}+\textstyle\sum_{n=1}^5\alpha_n^p cos(\frac{2n\pi t}{T}-\theta_n^p),\\
\left(\mu_n\left(\nabla\mathbf{u}+(\nabla\mathbf{u})^T\right)\right)\cdot\mathbf{n}&=0 \qquad \text{on } \partial\Omega_{out},
\end{aligned} \tag{5}$$

where A denotes the inlet cross section area of an artery, $\bar{Q}=59.09\ cm^3/min$, $\bar{p}=122.5\ mmHg$ are respectively the mean flow rate and mean pressure, T is the cardiac period, and the values of α_n^Q, α_n^p, θ_n^Q, and θ_n^p are listed in table I.

On the interface between the lumen and the porous wall, the pressure and velocity are assumed to be continuous across the interface. On other wall surface, the no-slip condition is applied. Thus to this end, the boundary value problem for the investigated problem is

BVP : Find $\mathbf{u}$, p_1, $\mathbf{v}$, p_2 such that (1)–(4) are satisfied in the computation domain $\Omega=\Omega_L\cup\Omega_W$ and all boundary conditions are satisfied.

III. METHOD OF SOLUTION

To develop the variational statement for the boundary value problem (BVP), we consider the following integral representation of the problem.

Find p_1, u_1, u_2, u_3 and p_2, v_1, v_2, v_3 ϵ H^1_Ω such that for all test functions $\hat{u}_i$ ϵ $H^1_{0u_i}(\Omega)$, $\hat{v}_i$ ϵ $H^1_{0v_i}(\Omega)$, and $\hat{p}_1$, $\hat{p}_2$ ϵ $H^1(\Omega)$, all the Dirichlet boundary conditions for the unknown functions are satisfied and

$$(\nabla\cdot\mathbf{u},\hat{p}_1)=0, \tag{6}$$

$$\begin{aligned}\rho\left(\tfrac{\partial\mathbf{u}}{\partial t}+\mathbf{u}\cdot\nabla\mathbf{u},\hat{\mathbf{u}}\right)-\left(\nabla\cdot\mu_n(\nabla\mathbf{u}+(\nabla\mathbf{u})^T),\hat{\mathbf{u}}\right)\\ +(\nabla p_1,\hat{\mathbf{u}})=(\mathbf{f},\hat{\mathbf{u}}),\end{aligned} \tag{7}$$

$$(\nabla\cdot\mathbf{v},\hat{p}_2)=0, \tag{8}$$

$$\begin{aligned}\left(\rho\ \tfrac{\partial\mathbf{v}}{\partial t}-\nabla\cdot\mu(\nabla\mathbf{v}+(\nabla\mathbf{v})^T),\hat{\mathbf{v}}\right)+\tfrac{\mu}{\kappa}(\mathbf{v},\hat{\mathbf{v}})\\ +(\nabla p_2,\hat{\mathbf{v}})=(\mathbf{g},\hat{\mathbf{v}}),\end{aligned} \tag{9}$$

where $(\cdot,\cdot)$ denotes the inner product on the square integrable function space $L^2(\Omega)$, $H^1(\Omega)$ is the Sobolev space $W^{1,2}(\Omega)$ with norm $\|\cdot\|_{1,2,\Omega}$, $H^1_{0u_i}(\Omega)=\{v\epsilon H^1(\Omega)|v=0$ on the boundary where u_i is specified$\}$. A standard procedure is then carried out to reduce the second-order derivatives involved in the above problem into the first-order ones using integration by parts to ensure that all integrals involved are well defined.

Through a Galerkin finite element formulation, we obtain the following system

$$\mathbf{M}\dot{\mathbf{U}}\ +\ \mathbf{K}\mathbf{U}\ =\ \mathbf{F}, \tag{10}$$

where $\mathbf{U}=(\mathbf{v}_f,\ \mathbf{v}_B,\ \mathbf{v}_w)^T$ in which $\mathbf{v}_f$ and $\mathbf{v}_w$ denote quantities in the lumen region and the porous wall region, and $\mathbf{v}_B$ represents quantities on the interface between the lumen region and the porous wall region.

A standard backward Euler scheme can then be used to solve the above system of ordinary differential equations to

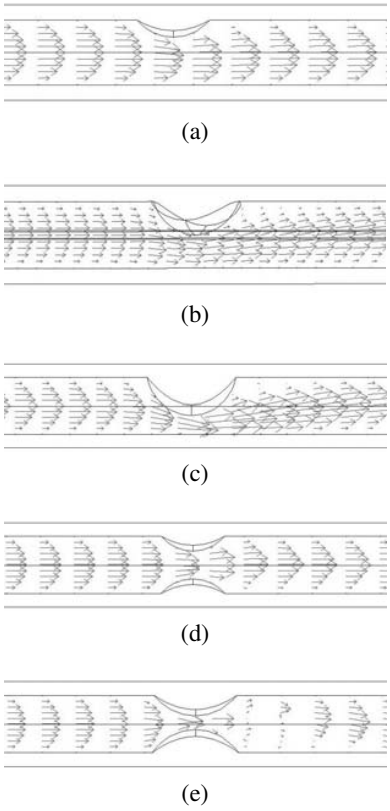

Fig. 3. Vector plots of the velocity fields in the luminal channel at the peak of systole of the non-Newtonian model (a) with 25% stenotic tube, (b) with 50% stenotic tube, (c) with 65% stenotic tube, (d) with symmetric type 50% stenotic tube, and (e) with symmetric type 80% stenotic tube.

determine the velocity and pressure fields at any instant of time.

IV. Results and Discussion

Using the numerical technique developed, a series of numerical experiments have been carried out to study the flow behaviour of blood through a porous medium stenosed artery and to investigate the significance of the non-Newtonian effect on blood flow for various cases of stenosis severity. Here, in this section, we present results for some of the investigated cases to demonstrate the essential features of the blood flow through the porous medium stenotic arteries and to show the significance of non-Newtonian effect on blood flow for the examined cases. Two different models, the Newtonian model and the non-Newtonian Carreau model, are used in the modelling. Various cases of stenosis severity, ranging from 25% to 80%, are considered. The computation domain is a straight tube of length of $5cm$ and the diameter of the lumen is $0.210cm$. The thickness of the wall is $0.05cm$. Two different types of stenoses, asymmetric and symmetric as shown in Fig. 3, are considered in this work. The blood density is $\rho = 1.06g/cm^3$, the Newtonian viscosity of blood is $0.0345g/(cm \cdot s)$, the parameters in the non-Newtonian Carreau model have values $\mu_0 = 0.56g/(cm \cdot s)$, $\mu_\infty = 0.0345g/(cm \cdot s)$, $\lambda = 3.313s$, and $n = 0.3568$, the parameters in the Brinkman equation have values $\mu = 0.0345g/(cm \cdot s)$, and $\kappa = 1.0e^{-14}cm^2$.

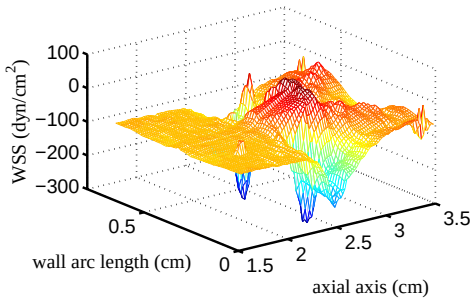

Fig. 4. Surface plot of wall shear stresses (WSS) on the 50% stenotic tube using the non-Newtonian model.

Fig. 3 shows the three-dimensional vector plots of the velocity field in the lumen region at the peak of systole obtained by using the Carreau model. The diagrams describe the general feature of blood flow through stenotic arteries with different degree of stenosis area-severity. It is noted that for the asymmetric case, when the stenosis area severity reaches 50%, a small flow recirculation zone occurs near the back toe of the stenosis where altherosclerotic diseases may develop.

To demonstrate the feature of wall shear stress distribution, we plot the wall shear stress on the plane representing the wall surface where the stenosis is located at the centre as shown in Fig. 4. It is noted that large magnitudes of wall shear stresses occur near the throat of the stenosis.

Fig. 5 shows the distributions of the axial velocity component u_x on three different cross sections of the 50% stenosed artery at the peak of systole $t = 3.15s$, obtained by both the Newtonian model and the non-Newtonian Carreau model. On the upstream cross section $x = 2cm$, the velocity profile is symmetric. On the downstream cross section $x = 2.7cm$, the velocity profile is no longer symmetric and there exists a small region with low velocity. The results also clearly show that, for the problem examined, the non-Newtonian property of blood has very significant effect on the velocity profiles particularly on the downstream cross section.

Fig. 6 shows the pressure distributions along the axial line (x-axis) at the peak of systole $t = 3.15s$, obtained by both the Newtonian model and the Carreau model. It is noted that the non-Newtonian behaviour only slightly affects the pressure distribution. The results also indicate that as the degree of the stenosis area severity increases, the pressure gradient required to impel the blood passing through the narrowing channel increases significantly. This results in a higher pressure to occur in the up-stream region.

Fig. 7 shows the effect of stenosis severity on blood pressure for the asymmetric case, obtained by using the non-Newtonian model. The results clearly show how blood pressure increases as the degree of the stenosis severity increases.

Fig. 8 shows the distributions of wall shear stresses (WSS) on three cross-sections of the 50% stenotic artery at the peak

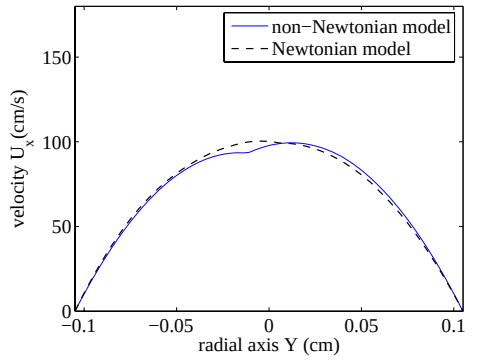

(a)

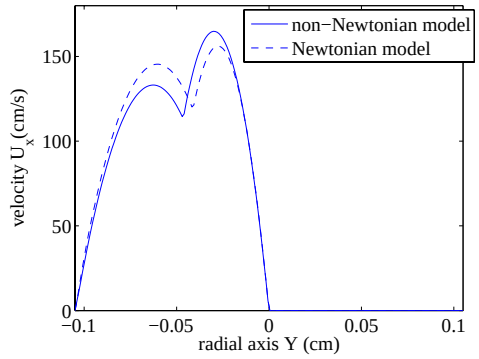

(b)

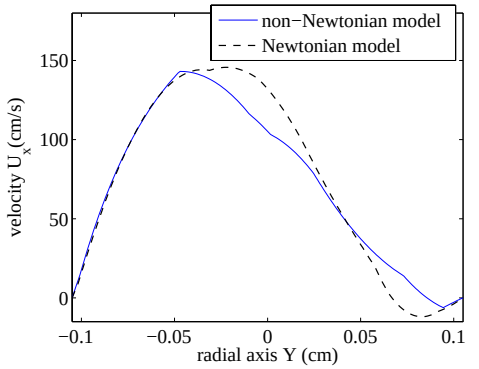

(c)

Fig. 5. The velocity field u_x in the lumen region of the 50% stenotic tube at the peak of systole $t = 3.15s$: (a) at an upstream cross section $x = 2.0\ cm$, (b) at the throat cross section $x = 2.5\ cm$, and (c) at a downstream cross section $x = 2.7\ cm$.

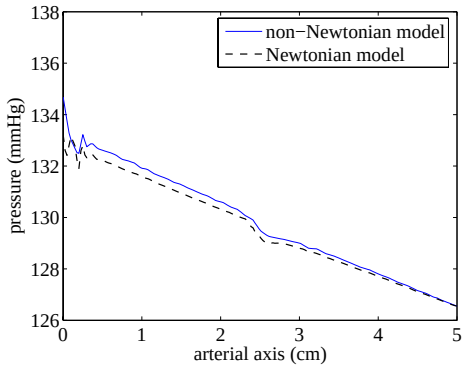

(a)

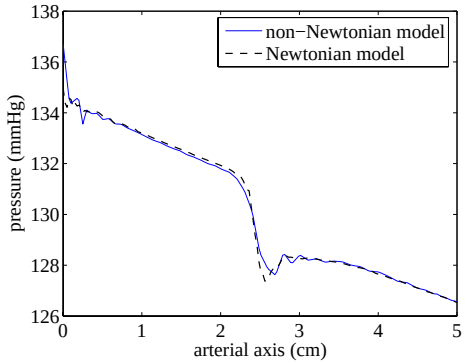

(b)

Fig. 6. Pressure along the axial line $(x, -0.05, 0)$ in the tube with different stenosis area severity at the peak of systole $t = 3.15s$: (a) 25%, and (b) 50%.

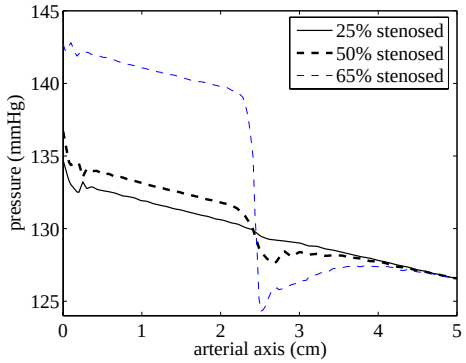

Fig. 7. Pressure along the axial line $(x, -0.05, 0)$ in the artery with different stenosis area severity at the peak of systole $t = 3.15s$, obtained by the non-Newtonian model.

of systole $t = 3.15s$, obtained by using the Newtonian model and the non-Newtonian Carreau model. It is clear that the non-Newtonian behaviour has very significant effect on the magnitude of wall shear stresses.

V. Conclusions

A numerical technique has been developed to simulate the three dimensional pulsatile blood flow in stenotic arteries and to study the effect of the non-Newtonian viscosity of blood on the flow behaviour. The results show that blood pressure increases very significantly in the upstream zone of the stenotic artery as the degree of the stenosis area severity increases. It is also shown that the non-Newtonian behaviour of blood has significant effects on the velocity profile of the blood flow and the magnitude of the wall shear stresses.

References

[1] F. Migliavacca, R. Yates, G. Pennati, G. Dubini, R. Fumero, and M. R. de Leval, "Calculating blood flow from doppler measurements in the systemic-to-pulmonary artery shunt after the norwood operation: a method based on computational fluid dynamics," *Ultrasound in Medicine and Biology*, vol. 26, pp. 209–219, 2000.

[2] F. Migliavacca, G. Dubini, G. Pennati, R. Pietrabissa, R. Fumero, T.-Y. Hsia, and M. R. de Leval, "Computational model of the fluid dynamics in systemic-to-pulmonary shunts," *Journal of Biomechanics*, vol. 33, pp. 549–557, 2000.

[3] F. Migliavacca, L. Petrini, M. Colombo, F. Auricchio, and R. Pietrabissa, "Mechanical behavior of coronary stents investigated through the finite element method," *Journal of Biomechanics*, vol. 35, pp. 803–811, 2002.

[4] M. Oshima, R. Torii, T. Kobayashi, N. Taniguchi, and K. Tukagi, "Finite element simulation of blood blow in the cerebral artery," *Computer methods in applied mechanics and engineering*, vol. 191, pp. 661–671, 2001.

[5] A. Redaelli, F. Boschetti, and F. Inzoli, "The assignment of velocity profiles in finite element simulations of pulsatile flow in arteries," *Computers in Biology and Medicine*, vol. 27, pp. 233–247, 1997.

[6] C. A. Taylor, T. J. Hughes, and C. K. Zarins, "Finite element modeling of blood flow in arteries," *Computer methods in applied mechanics and engineering*, vol. 158, pp. 155–196, 1998.

[7] K. Lee and X. Xu, "Modelling of flow and wall behaviour in a mindly stenosed tube," *Medical Engineering and Physics*, vol. 24, pp. 575–586, 2002.

[8] B. Liu and D. Tang, "A numerical simulation of viscous flows in collapsible tubes with stenose," *Applied Numerical Mathematics*, vol. 32, pp. 87–101, 2000.

[9] H. Jung, J. W. Choi, and C. G. Park, "Asymmetric flows of non-newtonian fluids in symmetric stenosed artery," *Korea-Australia Rheology Journal*, vol. 16, pp. 101–108, 2004.

[10] H. Hoogstraten, J. Kootstra, B. Hillen, J. Krijger, and P. Wensing, "Numerical simulation of blood flow in an artery with two successive bends," *Journal of Biomechanics*, vol. 29, pp. 1075–1083, 1996.

[11] T. Ishikawa, L. F. Guimaraes, S. Oshima, and R. Yamane, "Effect of non-Newtonian property of blood on flow through a stenosed tube," *Fluid Dynamics Research*, vol. 22, pp. 251–264, 1998.

[12] C. Tu and M. Deville, "Pulsatile flow of non-newtonian fluids through arterial stenoses," *Journal of Biomechanics*, vol. 29, pp. 899–908, 1996.

[13] M. Bonert, J. G. Myers, S. Fremes, J. Williams, and C. R. Ethier, "A Numerical Study of Blood Flow in Coronary Artery Bypass Graft Side-to-Side Anastomoses," in *Annals of Biomedical Engineering*, vol. 30, 2002, pp. 599–611.

[14] D.-Y. Fei, J. D. Thomas, and S. E. Rittgers, "The Effect of Angle and Flow Rate Upon Hemodynamics in Distal Vascular Graft Anatomoses: a Numerical Model Study," *Journal of Biomechanical Engineering*, vol. 116, pp. 331–336, 1994.

[15] M.-H. Song, M. Sato, and Y. Ueda, "Three-Dimensional Simulation of Coronary Artery Bypass Grafting with the Use of Computational Fluid Dynamics," *Surgery Today*, vol. 30, pp. 993–998, 2000.

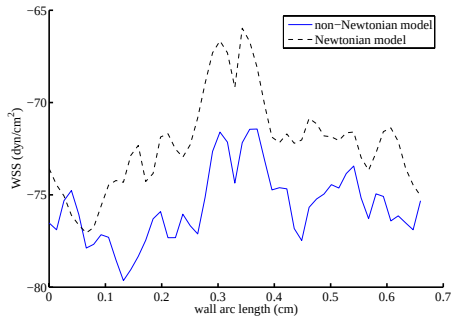

(a)

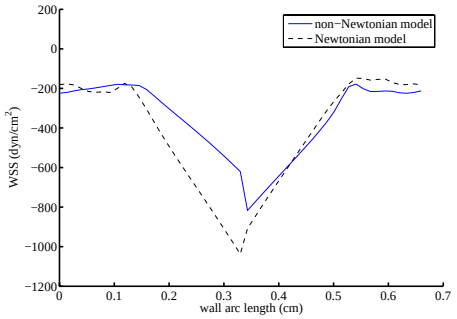

(b)

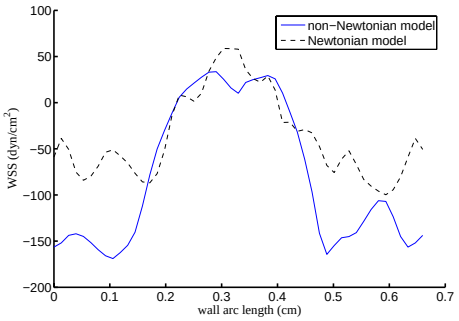

(c)

Fig. 8. Distribution of wall shear stresses(WSS) on three different cross sections of the 50% stenotic artery at the peak of systole $t = 3.15s$: (a) at $x = 2.0cm$, (b) at $x = 2.5cm$, and (c) at $x = 2.7cm$ (The stenosis is at the centre).